UNCLASSIFIED

AD 400 340

Reproduced
by the

ARMED SERVICES TECHNICAL INFORMATION AGENCY
ARLINGTON HALL STATION
ARLINGTON 12, VIRGINIA

UNCLASSIFIED

NOTICE: When government or other drawings, specifications or other data are used for any purpose other than in connection with a definitely related government procurement operation, the U. S. Government thereby incurs no responsibility, nor any obligation whatsoever; and the fact that the Government may have formulated, furnished, or in any way supplied the said drawings, specifications, or other data is not to be regarded by implication or otherwise as in any manner licensing the holder or any other person or corporation, or conveying any rights or permission to manufacture, use or sell any patented invention that may in any way be related thereto.

63-3-1

400340

400 340

ASTIA

APR 9 1963

TISIA A

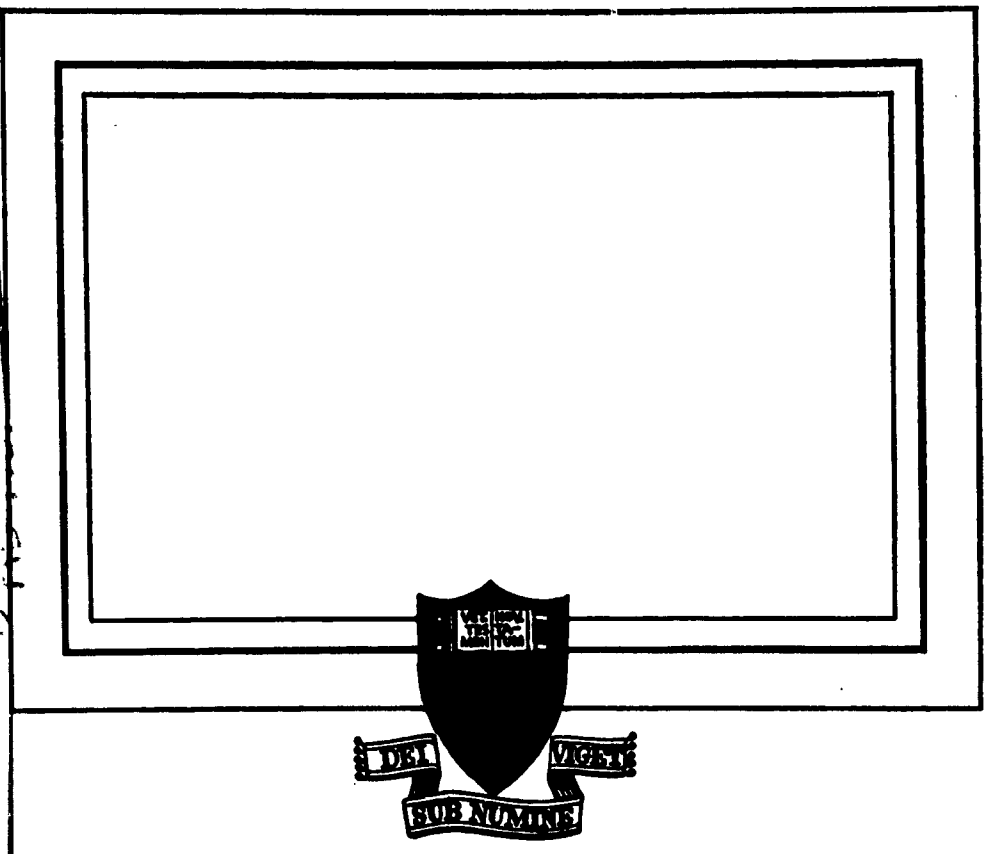

PRINCETON UNIVERSITY

Princeton University
ONR Contract Nonr 1858(27)
NR-014-203

Technical Report No. 13

INTERMOLECULAR POTENTIAL IN SOLID METHANE.

I. INFLUENCE ON THE VIBRATIONAL SPECTRUM AND THE CRYSTAL STRUCTURE.

by

S. Kimel, A. Ron, and D. F. Hornig

February 1963

INTRODUCTION

The infrared spectra of crystalline CH_4 and CD_4 in all phases have recently been studied by Savitsky and Hornig[1]. In the low-temperature phase II spectra of

---

1. G. B. Savitsky and D. F. Hornig, J. Chem. Phys. 36, 2634 (1962).

---

pure CH_4 or CD_4 they observed fine structure in the bending region ν_4 (three peaks separated by two intervals of 4 cm^{-1} each, the peak at the lowest frequency being extremely weak) and essentially a single peak in the stretching region, ν_3. The spectra of dilute solid solutions of both isotopic species in one another consist of single bands with half widths ≤ 3 cm^{-1}. The relevant spectra are reproduced in Figure 1.

These observations indicate that the splittings in the spectra of the pure crystals arise from dynamic intermolecular interactions rather than from statie interactions which would show up also in dilute solutions.

There are many structures for methane crystals that would split an F mode into two or three infrared active components. The D_{2d}^2 and D_{2d}^3 space groups with 2 molecules per unit cell, or the D_{2d}^{11} space group having the same packing with one molecule per unit cell were found to be the most probable structures since they represent the most efficient hydrogen packing.

All present calculations apply to the D_{2d}^2 as well as the D_{2d}^3 structure. The latter is less likely since it would allow the molecular A and E modes to become active in the crystal and they have not been observed.

It may seem that in these structures both molecules in the unit cell are parallel (see Figure 2) thus yielding a structure with one molecule per unit cell, namely D_{2d}^{11}. However, small distortions are sufficient to retain the model of two molecules per unit cell. In the D_{2d}^{11} structure the molecular F modes are split into doublets rather than into triplets. This fact, taken alone, does not invalidate the D_{2d}^{11} structure since one peak in the observed spectra is so weak as to be uncertain.

Intermolecular Potential in Solid Methane

I. Influence on the Vibrational Spectrum and the Crystal Structure

by

S. Kimel*, A. Ron, and D. F. Hornig
Frick Chemical Laboratory, Princeton University, Princeton, N. J.

ABSTRACT

The spectrum of the low-temperature phase of crystalline methane has been calculated using a model of atom-atom interactions consisting of repulsive, attractive, and electrostatic parts V_R, V_A, and V_E. Detailed calculations were carried out for the D_{2d}^2 and D_{2d}^{11} structures previously suggested for phase II of crystalline methane. Using potentials derived from other sources, it is possible to infer a potential for methane which yields partial agreement between the calculated and observed spectra. In accordance with observations it is found that the calculated coupling splitting in the stretching region and all site splittings are small enough to be included in the experimental band widths. In the bending region of the pure crystal spectrum the calculated spacings between the lines in the triplet agree with experiment but the model fails to account for the intensity pattern and also for the frequency shifts of the solid solutions in either region.

*On leave of absence: Weizmann Institute of Science, Rehovoth, Israel.

According to group theory each structure predicts the same number of infrared active bands for both F modes in pure crystals as well as solid solutions (See Table I).

To reconciliate the group theoretical predictions with experimental results it is required that the numerical results for the splittings should be such that the coupling splittings in the bending region are larger than in the stretching region and also larger than all site splittings.

In this study the site and coupling splittings are calculated for the D_{2d}^{2} and D_{2d}^{11} structures. The calculations are based on a model of atom-atom interactions recently introduced by Dows[2,3,4].

---

2. D. A. Dows, J. Chem. Phys. 32, 1342 (1960).

3. D. A. Dows, J. Chem. Phys. 35, 282 (1961).

4. D. A. Dows, J. Chem. Phys. 36, 2836 (1962).

GENERAL CONSIDERATIONS

In this section the calculation of absorption frequencies of molecular crystals is outlined and applied to the case of methane. Intermolecular force constants for the vibrational modes in the crystal are derived for an appropriate intermolecular potential and the secular equation for the unit cell is solved.

The following simplifications are made:

1. No mixing of stretching and bending modes, e.g. the hydrogens move along or perpendicular to the C-H bonds.
2. No librations.
3. The methane molecules in the crystal have essentially T_d symmetry.
4. The tetragonal unit cell is based on a face-centered cubic symmetry.

These assumptions enable us to solve the problem in a first approximation without computational difficulties.[5] At this stage it does not seem justified to

---

5. All calculations were carried out without explicitly taking into account carbon recoil. In a later section, however, the influence of carbon recoil on the calculated spectrum is discussed qualitatively.

---

refine the model before more information is available about forces acting in molecular crystals. We are currently investigating the influence on the spectrum of a change in the symmetry of the molecules and also of the unit cell.

Symmetry Coordinates

Symmetry coordinates, S^{cr}, for the doubly occupied D_{2d}^{2} unit cell are built from normal coordinates, Q, of individual methane molecules. With the assumption of "no mixing", molecular normal coordinates are simply proportional to molecular symmetry coordinates with proportionality factors L_{33} for the stretching mode and L_{44} for the bending mode.

Results for the singly occupied D_{2d}^{11} unit cell can be obtained in a trivial way from the D_{2d}^{2} structure. Therefore the formalism will not be worked out separately.

From group theoretical considerations it follows that each F mode of the individual molecules gives rise to three infrared active modes in the crystal, as summarized in Table I.

Table I

Correlation of the Isolated Tetrahedron and the Tetrahedron in the Crystal*

Molecular Symmetry	Site Symmetry	Space Group Symmetry
T_d	D_2	D_{2d}^{2}
$\underline{F_2}$	$\underline{B_1}$ (z)	A_2 (z)
		$\underline{B_2}$ (z)
	$\underline{B_2}$ (y)	$\underline{2E}$ (x,y)
	$\underline{B_3}$ (x)	

*Underlined species are infrared active.

If we denote the two molecules in the unit cell as p and q (see Figure 2), then the symmetry coordinates, S^{cr}, for the unit cell may formally be written as

$$
\begin{aligned}
S^{cr}(B_2) &= \left\{Q_p(F_z) + Q_q(F_z)\right\}2^{-1/2} \\
S^{cr}(A_2) &= \left\{Q_p(F_z) - Q_q(F_z)\right\}2^{-1/2} \\
S^{cr}(E_+) &= \left\{Q_p(F_{x,y}) + Q_q(F_{x,y})\right\}2^{-1/2} \\
S^{cr}(E_-) &= \left\{Q_p(F_{x,y}) - Q_q(F_{x,y})\right\}2^{-1/2} \ .
\end{aligned} \tag{1}
$$

There are two sets of coordinates: one built from the bending modes F_x, F_y, F_z and another set from the stretching modes F_x, F_y, F_z. In the free molecule the F_x, F_y, and F_z modes are degenerate but in a non-cubic crystal they may be different. As indicated in Equations (1) the $S^{cr}(E)$ modes can be built either from $Q(F_x)$ or from $Q(F_y)$.

Shifts and Splittings

In order to calculate the frequencies of the unit cell modes the force constant matrix for the unit cell is introduced

$$
\begin{bmatrix}
\lambda_o + f_{pp} & f_{pq} \\
f_{pq} & \lambda_o + f_{pp}
\end{bmatrix}
$$

The G matrix in this notation is the identity matrix. Solving the secular equation for λ we obtain for the F stretching and bending modes

$$
\begin{aligned}
\lambda(B_2) &= \lambda_o + f_{pp}[Q(F_z)] + f_{pq}[Q(F_z)] \\
\lambda(A_2) &= \lambda_o + f_{pp}[Q(F_z)] - f_{pq}[Q(F_z)] \\
\lambda(E_+) &= \lambda_o + f_{pp}[Q(F_{x,y})] + f_{pq}[Q(F_{x,y})] \\
\lambda(E_-) &= \lambda_o + f_{pp}[Q(F_{x,y})] - f_{pq}[Q(F_{x,y})] \ .
\end{aligned} \tag{2}
$$

Here $\lambda_o = 4\pi^2c^2\nu_o^2$ for the isolated molecule and thus contains all intramolecular interactions,

$$
f_{pp} = \frac{\partial^2 V}{\partial Q_p^2} + \frac{\partial^2 V}{\partial Q_p \partial Q_{p'}} \tag{3}
$$

and

$$
f_{pq} = \frac{\partial^2 V}{\partial Q_p \partial Q_q} \ . \tag{4}
$$

V is the intermolecular potential, which corresponds to the term $\Sigma_i \Sigma_j V_{ij}$ in the general expression for the potential energy given by Hornig[6]. This part of the

6. W. Vedder and D. F. Hornig, Advances in Spectroscopy 2, 189 (1961).

potential contains cross terms between internal coordinates of all molecules.

The expressions (2) for λ show, for each crystal mode, that λ depends on three terms. These are λ_o, the gas value for that mode, the term f_{pp} which produces a shift and finally a term f_{pq} which produces a splitting,

$$\Delta\lambda_{coupling} = f_{pq} \cdot \tag{5}$$

The coefficient f_{pp} in Equation (2) contains two terms. The first (the second derivative with respect to the normal coordinate Q of molecule p) is a static perturbation, while the second or "exchange" term (the derivative with respect to coordinate Q of molecule p and of another molecule p' which is translationally equivalent to p) is a dynamic perturbation. In dilute solid solutions of one isotopic species in another $f_{pq} = 0$ and also the second term of f_{pp} vanishes, since at low concentrations all neighbors are of the other species and do not cause dynamic perturbations. Hence the values of λ in a solid solution, λ_{ss}, are shifted with respect to the gas value by amounts

$$\lambda_{ss} - \lambda_o = \partial^2 V / \partial Q_p^2 \cdot \tag{6}$$

It should be noted that values for $\Delta\lambda_{coupling}$ do not occur around λ_{ss} but rather around the (non observable) value $\lambda_{crystal}$, which is defined by Equations (3) and (6) as

$$\lambda_{crystal} = \lambda_{ss} + \partial^2 V / \partial Q_p \partial Q_{p'} \cdot \tag{7}$$

For the D_{2d}^{11} structure with one molecule in a unit cell on the D_{2d} site we expect two lines in the solid solution, due to different static shifts in the z and x,y directions

$$\lambda_{ss}(z) = \lambda_o + \partial^2 V / \partial Q^2 (F_z)$$

$$\lambda_{ss}(x,y) = \lambda_o + \partial^2 V / \partial Q^2 (F_{x,y}) \cdot$$

In the pure crystal there will now be two lines due to different static plus dynamic shifts in the z and x,y directions

$$\lambda(B_2) = \lambda_o + \partial^2V/\partial Q^2(F_z) + \partial^2V/\partial Q(F_z)\partial Q'(F_z)$$

$$\lambda(E) = \lambda_o + \partial^2V/\partial Q^2(F_{x,y}) + \partial^2V/\partial Q(F_{x,y})\partial Q'(F_{x,y}) ,$$

where Q' indicates a normal coordinate in a neighboring molecule.

The pure crystal lines are the lines $\lambda(B_2)$ and $\lambda(E_+)$ in the D^2_{2d} structure. The solid solution spectra are identical for both structures.

INTERMOLECULAR POTENTIAL

In methane crystals the intermolecular potential which influences the vibrational frequencies is expected to be mainly due to interactions between non-bonded hydrogens. Furthermore, intermolecular interactions between hydrogens and carbons may contribute considerably to all static shifts.

For this case the intermolecular potential can be written in the form

$$V = \sum_i \sum_j V_{ij}(R_{ij}) + \sum_i \sum_k V_{ik}(R_{ik}) , \qquad (8)$$

where R, the distance between hydrogen i of a given molecule and hydrogen j or carbon k of a neighboring molecule are expressed in Angstrom units and V in ergs.

The distances R are determined by the geometry of the crystal which is schematically drawn in Figure 2. As an example consider hydrogen 1 of molecule p, or p1. It has four nearest hydrogens, labeled j = 1,2,3,4, at distances $R_{ij} = R_f = 2.77A$; these are q4, q3, (q-a)3, (q-b)4. Furthermore, there are six next-nearest hydrogens, labeled j = 5,6,7,8,9,10, at distances $R_{ij} = R_g = 3.13A$. Two of these hydrogens [q2 and (q-c)2] belong to type q molecules, while the other four hydrogens [(p+a)2, (p+a)4, (p+b)2, (p+b)3] belong to translationally equivalent molecules p' of type p[7].

---

7. This distinction which exists, of course, only in the D^2_{2d} or D^3_{2d} structures is carried through all the calculations. For the D^{11}_{2d} structure corresponding terms involving p and q molecules are combined.

The classification of neighbor hydrogens is continued till all hydrogens (69 in total) within a radius of 6A from atom p1 are labeled as is shown in Figure 2 and

Appendix III. Similarly all carbon contacts within a radius of 6A from hydrogen pl (16 in total) were considered (see Appendix IV). The cut-off at 6A for atom-atom interactions contributing to the potential (8) is somewhat arbitrary. However, during the course of the calculations it was seen that although at separations of 6A the interactions in some cases may remain important (see Tables II and III) their contribution to intermolecular force constants become quite small. In the present study index i in Equation (8) goes from 1 to 4, index j from 1 to 69 and index k from 1 to 16.

According to Equations (3) and (4) derivatives of the type $\partial^2 V/\partial Q^2$ have to be calculated. For hydrogen-hydrogen interactions, for example, V is defined in Equation (8) as an explicit function of R_{ij}. Hence we write for any mode Q

$$\frac{\partial^2 V}{\partial Q_p^2} = \left[\frac{\partial^2 V}{\partial R_{ij}^2}\left(\frac{\partial R_{ij}}{\partial \rho_i}\right)^2 + \frac{\partial V}{\partial R_{ij}}\frac{\partial^2 R_{ij}}{\partial \rho_i^2}\right]\left(\frac{\partial \rho_i}{\partial S_p}\frac{\partial S_p}{\partial Q_p}\right)^2 \qquad (9a)$$

$$\frac{\partial^2 V}{\partial Q_p \partial Q_q} = \left[\frac{\partial^2 V}{\partial R_{ij}^2}\frac{\partial R_{ij}}{\partial \rho_i}\frac{\partial R_{ij}}{\partial \rho_j} + \frac{\partial V}{\partial R_{ij}}\frac{\partial^2 R_{ij}}{\partial \rho_i \partial \rho_i}\right]\frac{\partial \rho_i}{\partial S_p}\frac{\partial S_p}{\partial Q_p}\frac{\partial \rho_j}{\partial S_q}\frac{\partial S_q}{\partial Q_q} \qquad (9b)$$

and similarly for $\partial^2 V/\partial Q_p \partial Q_p$, .

Here $\vec{\rho_i}$ and $\vec{\rho_j}$ are normal displacements of hydrogens i or j. In the approximation of "no mixing" $\vec{\rho}$ is along the C-H bonds for the stretching mode and for the bending mode $\vec{\rho}$ is perpendicular to the C-H bond in the proper plane. The factors $\partial\rho/\partial S$ are elements of the matrix [U'] which transforms molecular symmetry coordinates, S, into internal coordinates Δr and $\Delta\alpha d$ (see Appendix I). Δr is the change of the C-H bond length in the stretching mode, d = 1.093A is the equilibrium C-H bond length and α is the tetrahedral angle. In the calculations it is convenient to express internal coordinates in terms of $\theta = \alpha/2$. The factors $\partial S/\partial Q$ are elements of the matrix [L] which transforms molecular normal coordinates, Q, into symmetry coordinates S.

As mentioned before hydrogen-carbon interactions contribute to the shifts. This can be expressed by terms similar to those in Equation (9a) where all j are replaced by k and where V now stands for the hydrogen-carbon potential.

The intermolecular potential in solid methane can be separated into three contributions. First there is a repulsive potential of the form $V_R = a \exp(-bR)$. The parameters a and b are not known for atom-atom interactions in crystalline methane. V_R^{HH} may be taken from the function calculated by de Boer[8] for the

8. J. de Boer, Physica 9, 363 (1942).

exchange repulsion between non-bonded H atoms in hydrogen. Since it is derived for a specific case the de Boer function cannot be expected to apply rigorously in solid methane. Nevertheless it has been used with partial success for calculating the vibrational spectra of CH_3Cl[2,3], C_2H_4[4], and paraffin crystals.[9]

9. R. Snyder, J. Mol. Spectroscopy 7, 116 (1961).

Another expression used in the calculations for V_R^{HH}, given by Muller[10], is based on

10. A. Muller, Proc. Roy. Soc. (London) A 178 , 227 (1941).

the measured compressibilities of solid paraffins.

The repulsive potential between hydrogens and carbons was estimated to be $(V_R^{CC} \cdot V_R^{HH})^{1/2}$ where the C-C repulsive potential was taken to be equal to that between two Ne atoms[11] $V_R^{CC} = 2570 \times 10^{-12} \exp(-4.26\ R)$.

11. J. O. Hirschfelder, C. F. Curtiss, and R. B. Bird, Molecular Theory of Gases and Liquids (John Wiley and Sons, Inc., New York, 1954).

Using the de Boer function one obtains for the repulsive potential

$$V_R = V_R^{HH} + V_R^{HC}$$
$$= [120 \exp(-3.54\ R_{ij}) + 555 \exp(-3.90\ R_{ik})] \times 10^{-12} \text{ erg} \qquad (10a)$$

and with the Muller function one obtains

$$V_R' = [4400 \exp(-5.0\ R_{ij}) + 3360 \exp(-4.63\ R_{ik})] \times 10^{-12} \text{ erg} . \qquad (10b)$$

Secondly there is an attractive van der Waals type interaction of the form

$$V_A = V_A^{HH} + V_A^{HC} = -c\ R_{ij}^{-6} - c' R_{ik}^{-6} .$$

The coefficients c and c' were taken from a calculation by Pitzer and Catalano[12]

12. K. S. Pitzer and E. Catalano, J. Am. Chem. Soc. 78, 4844 (1956).

based on the dispersion force formulation of constituent atoms in hydrocarbons

$$V_A = [-3.42\ R_{ij}^{-6} - 8.68\ R_{ik}^{-6}] \times 10^{-12}\ (\text{erg}). \qquad (11)$$

A value of c, about twice as large, is found from calculation of the dispersion interaction between two H atoms[13] but it should be noted that this is quite a

13. C. Mavroyannis and M. J. Stephen, Mol. Phys. 5, 629 (1962).

different case.

In addition to the short-range potential of the Corner-Buckingham type[11], represented by Equations (10) plus (11), there are also long-range interactions arising from the charge distribution in the methane molecules. This may be regarded as an electrostatic interaction of the form $V_E = e_{eff}^2\ R^{-1}$ between electrical charges on non-bonded atoms.[14]

14. D. F. Hornig and G. L. Hiebert, J. Chem. Phys. 27, 752 (1957).
C. Haas and D. F. Hornig, J. Chem. Phys. 32, 1763 (1960).

Usually this type of interaction is treated as a transition-dipole interaction[2,3,4,9,15,16]

15. J. C. Decius et al, J. Chem. Phys. 22, 1941, 1946 (1954); 23, 1290 (1955) 25,1184 (1956).

16. R. M. Hexter, J. Chem. Phys. 33, 1833 (1960).

The effective charges, e_{eff}, can be estimated from intensities of infrared absorption bands in the solid state, which for methane have not been measured. For the gas phase the average values of e_{eff} derived from absolute band intensities[17]

17. R. Rollefson and R. Havens, Phys. Rev. 57, 710 (1940).
A. M. Thorndike, J. Chem. Phys. 15, 868 (1947).
H. L. Welsh et al, J. Chem. Phys. 19, 340 (1951); 20, 1646 (1952).
Spectrochim. Acta 16, 840 (1960).
J. Heicklen, Spectrochim. Acta 17, 201 (1961).

are about 0.12 e and about 0.06 e for ν_3 and ν_4 respectively, where e is the electronic charge. It is often observed that in going from the gas phase to the solid phase the intensities of infrared absorptions increase, particularly for the bending modes. This has been demonstrated for the case of benzene[18] and ethylene[19].

---

18. J. L. Hollenberg and D. A. Dows, J. Chem. Phys., in press.

19. G. M. Wieder and D. A. Dows, J. Chem. Phys. 37, 2990 (1962).

While Savitsky and Hornig[1] did not measure absolute intensities, Γ, of the infrared bands in solid methane it can be seen from their spectra that the ratio of intensities, $\Gamma(\nu_4)/\Gamma(\nu_3)$, measured on the same samples is larger than the ratio for intensities in the gas phase. The value $e_{eff} = 0.1$ e was initially chosen for both modes in methane. Hence

$$V_E = V_E^{HH} + V_E^{HC}$$

$$= [(0.1\ e)^2 R_{ij}^{-1} - (0.1\ e)(0.4\ e)R_{ik}^{-1}]10^{+8}\ (erg). \qquad (12)$$

In addition calculations were made with $e_{eff} = 0.07$ e and also with $e_{eff} = 0.14$ e to compensate for the lack of an experimental value for e_{eff} in the solid state.

The first and second derivatives with respect to R of the specific potentials (10, 11, 12) are numerical constants depending only on R. They are listed in Tables II and III for all interatomic contacts in crystalline methane for which $R < 6$A.

CALCULATIONS AND RESULTS

The numerical values for the individual factors in Equations (9) will now be discussed in detail.

a) The factors $\partial\rho/\partial s$.

We choose a coordinate system for the methane molecule such that the x, y, and z coordinates coincide with the three 2-fold axes in the molecule. In the approximation of "no mixing" the molecular symmetry coordinates are

$$S^{st}(A) = (\Delta r_1 + \Delta r_2 + \Delta r_3 + \Delta r_4)2^{-1}$$

$$S^{bd}(A) = d(\Delta\alpha_{12} + \Delta\alpha_{13} + \Delta\alpha_{14} + \Delta\alpha_{23} + \Delta\alpha_{24} + \Delta\alpha_{34})6^{-1/2}$$

$$S^{bd}(E_a) = d(2\Delta\alpha_{12} - \Delta\alpha_{13} - \Delta\alpha_{14} - \Delta\alpha_{23} - \Delta\alpha_{24} + 2\Delta\alpha_{34})12^{-1/2}$$

$$S^{bd}(E_b) = d(-\Delta\alpha_{13} + \Delta\alpha_{14} + \Delta\alpha_{23} - \Delta\alpha_{24})2^{-1}$$

$$S^{st}(F_x) = (\Delta r_1 - \Delta r_2 + \Delta r_3 - \Delta r_4)2^{-1}$$

$$S^{st}(F_y) = (\Delta r_1 - \Delta r_2 - \Delta r_3 + \Delta r_4)2^{-1}$$

$$S^{st}(F_z) = (\Delta r_1 + \Delta r_2 - \Delta r_3 - \Delta r_4)2^{-1}$$

$$S^{bd}(F_x) = d(\Delta\alpha_{13} - \Delta\alpha_{24})2^{-1/2}$$

$$S^{bd}(F_y) = d(\Delta\alpha_{14} - \Delta\alpha_{23})2^{-1/2}$$

$$S^{bd}(F_z) = d(\Delta\alpha_{12} - \Delta\alpha_{34})2^{-1/2}$$

The factors $\partial\rho/\partial S$ are elements of the matrix [U'] which is given in Appendix I.

b) The factors $\partial S/\partial Q$.

The factors $\partial S/\partial Q$ are elements of the matrix [L]. In the approximation of no mixing

$$L = (\lambda/F)^{1/2} = G^{1/2} , \qquad (13)$$

where F and G have the usual meaning in the Wilson notation.[20] This results in

---

20. E. B. Wilson, J. C. Decius, and P. C. Cross, Molecular Vibrations, McGraw-Hill, Inc., New York, 1955.

$$L_{33} = (\mu_H + 4\mu_C/3)^{1/2} = 1.050 \text{ (amu)}^{-1/2}$$

$$L_{44} = (2\mu_H + 16\mu_C/3)^{1/2} = 1.558 \text{ (amu)}^{-1/2} .$$

More accurate values may be obtained by inverting the complete matrix $[L^{-1}]$ given by Mills[21]. This results in

---

21. I. M. Mills, Mol. Phys. 1, 107 (1958).

$[L]_{F_2}$ (amu)$^{-1/2}$

	Q_3	Q_4
S_3	1.0497	-0.0342
S_4	-0.1612	1.5499

The "no mixing" assumption seems to be justified by the smallness of the off-diagonal terms and by the numerical agreement between the diagonal elements in the [L] matrix and the values for L_{33} and L_{44} obtained with Equation (13).

c) The derivatives of R_{ij} and R_{ik}

Calculations of the derivatives $\partial R/\partial\rho$, $\partial^2 R/\partial\rho_i^2$ and $\partial^2 R/\partial\rho_i\partial\rho_j$ involved most of the computational work. The expressions for the distances R_{ij} between atom pl and 69 neighboring hydrogens were differentiated with respect to Δr_i, Δr_j, $\Delta\theta_{12}$, $\Delta\theta_{13}$, $\Delta\theta_{12}$ (or $\Delta\theta_{34}$), $\Delta\theta_{13}$ (or $\Delta\theta_{24}$) resulting in 414 values for $\partial R_{ij}/\partial\rho$ and also 414 values for the second derivatives which are collected in Appendices III and IV respectively.[22]

---

22. Δr_i and $\Delta\theta.d$ are normal displacements of atom pl, while Δr_j and $\Delta\theta'.d$ are normal displacements of hydrogens in neighboring molecules.

The carbon neighbors contribute mainly to the static shifts. Hence the expressions for the distances R_{ik} between hydrogen pl and 16 neighboring carbons were differentiated with respect to Δr_i, $\Delta\theta_{12}$, and $\Delta\theta_{13}$ resulting in 48 values for $\partial R_{ik}/\partial\rho_i$ and also 48 values for $\partial^2 R_{ik}/\partial\rho_i^2$. These are collected in Appendix V.

A convenient way[2] to calculate derivatives of this type is through the following trigonometric relations

$$\frac{\partial R_{ij}}{\partial\rho_i} = \cos(\vec{R}_{ij},\vec{\rho}_i) = \frac{\vec{R}_{ij}\cdot\vec{\rho}_i}{|R_{ij}||\rho_i|} \qquad (14)$$

and

$$\frac{\partial^2 R_{ij}}{\partial\rho_i\partial\rho_j} = \frac{\sin(\vec{R}_{ij},\vec{\rho}_i)\sin(\vec{R}_{ij},\vec{\rho}_j)\cos\gamma}{|R_{ij}|}$$

$$= \frac{(\vec{\rho}_i \times \vec{R}_{ij})\cdot(\vec{R}_{ij} \times \vec{\rho}_j)}{|R_{ij}|^3\,|\rho_i|\,|\rho_j|} \quad , \qquad (15)$$

where γ is the dihedral angle formed by the three vectors $\vec{R}_{ij}$, $\vec{\rho}_i$, and $\vec{\rho}_j$.

The direction cosines of $\vec{R}_{ij}$ can be expressed straightforwardly in terms of the parameters h, d, and θ (see Figure 2). The direction cosines of $\vec{\rho}$ are elements of the molecular matrix [D] which transforms cartesian coordinates into

internal coordinates and which is given in Appendix II.

d) Results

We now substitute into Equations (9) the values obtained above for the various factors (except $\partial S/\partial Q = L$) and take the appropriate sums over all contacts as listed in Appendices VI - IX.

Intermolecular force constants for H-H and H-C interactions obtained with the three types of potentials considered in the foregoing section are listed in Table IV. The terms involving $\partial V/\partial R$ and $\partial^2 V/\partial R^2$ are listed separately in order to show that they are of about equal importance. For the repulsive potential (10) it may seem that the terms with $\partial V/\partial R$ are smaller by a factor $bR \sim 10$. For this and other reasons terms with $\partial V/\partial R$ have not been included in previous calculations.[2,3,4,9]

Results for the shifts and splittings (in cm^{-1}) are obtained from the force constants f through the relation

$$\Delta\upsilon = fL^2/(8\pi^2 c^2 \upsilon_0) \ . \qquad (16)$$

In the stretching region ($\upsilon_3 = 3019\ cm^{-1}$) 100 dyne cm^{-1} is equivalent to 0.31 cm^{-1}, while in the bending region ($\upsilon_4 = 1306\ cm^{-1}$) 100 dyne cm^{-1} is equivalent to 1.56 cm^{-1}.

From Equation (16) it follows that for a given value of f the resulting value of $\Delta\upsilon$ in the bending region will be larger than in the stretching region by a trivial factor $(F_{33}G_{44}/F_{44}G_{33})^{1/2}$ which for υ_4 and υ_3 of methane equals about 5.

Final results for calculated shifts and splittings are listed in Table V. Here we considered all combinations of the three types of intermolecular potentials given above. For the repulsive potential these are: the deBoer potential V_R and the Muller potential $V_{R'}$. For the electrostatic potential these are V_E, $2V_E$ and $V_E/2$. For completeness the attractive potential was varied between[12] V_A and $2V_A$ although the latter value[13] was derived for a considerably different system.

The sum of all attractive and repulsive atom-atom interactions may be

regarded as a measure of the lattice energy. This can be compared to the known value of the heat of sublimation for crystalline methane which is[23]

---

23. Handbook of Chemistry and Physics, Chemical Rubber Publishing Co., Cleveland, O.

2240 cal/mole = 1700 x 10^{-16} erg/molecule.

Good agreement is obtained for the combinations $(V_R + V_A)$ and $(V_{R'} + V_A)$ yielding respectively 1660 and 2080 x 10^{-16} erg/molecule. The combinations involving $2V_A$ yield values for the lattice energy which are too large by a factor 2 or more. Due to symmetry considerations the electrostatic potential V_E does not contribute to the lattice energy. This was checked numerically for the 12 neighbors arranged cubically around molecule p and indeed it was found that $V_E^{HH} + V_E^{CC} = - V_E^{HC}$.

DISCUSSION OF RESULTS

We now summarize the results obtained with the present calculations and compare them with experiment.

In good agreement with the observations are the following results:

1) In the bending region the calculated site splitting for all cases (except 7) are small enough so they may very well be included in the band widths. In the stretching region the site splitting is identically zero.
2) The coupling splitting in the stretching region in all cases is also small enough to be accounted for by the measured band widths.
3) The coupling splitting in the bending region is of about the right magnitude for cases 5, 6 or 10 if we assume two molecules per unit cell. For one molecule per unit cell the additional combinations 2 and 12 become applicable.

However, the positions of the two components B_2 and E_+ are not in agreement with the previous assignment[1]. The latter was based on intensity considerations in the observed spectrum, according to which B_2 should be on the low-frequency side of E_+.

The partial agreement between experimental and calculated results seems to verify the basic assumptions made at the start of this work about the packing in methane crystals and about the possibility of interpreting the observed spectra using a model of atom-atom interactions.

The present treatment does not allow us to draw definite conclusions about the parameters in the intermolecular potential. Out of the combinations 2, 5, 6, 10, and 12 which yield reasonable splittings for CH_4, 5 gives the best result for the lattice energy. The fact that the calculated site splitting for this case is only barely acceptable can easily be rectified by increasing V_A somewhat.

Very little can be said at this stage about the shifts. Both the observed and calculated solid solution shifts for CH_4 show (for cases 1, 3, 5, 7, 9, and 11) that the shifts in the stretching region are about 6 cm^{-1} toward the red compared to the corresponding shifts in the bending region (see Table V). The experimental shifts may be obtained by adding to the calculated values, red shifts of about 8 cm^{-1} for the stretching as well as the bending mode. These may be due to various factors such as carbon-carbon interactions, the dielectric medium or anharmonic effects which are poorly known.[4,21]

---

21. D. F. Ball and D. C. McKean, Spectrochim. Acta 18,1029 (1962).

Deutero-methane

We now apply the present calculations to the case of deutero-methane. In comparing CH_4 with CD_4 we first assume the crystal structure, the force field and the geometrical factors to be identical. The different masses of H and D give rise to different gas frequencies, ν_o, and also to different elements in the matrix [L], which in turn enter the results through Equation (16). If we neglect the carbon movements in the lattice, then the matrices [D] for the isotopic species are identical. In this approximation all calculated shifts and splittings for CD_4 will be smaller than for CH_4 by a factor

$$(L^2_D/L^2_H)(\nu_o{}^H/\nu_o{}^D) = (G_D/G_H)^{1/2} . \qquad (17)$$

For the bending region this results in a 23 °/o decrease of all calculated values. For the solid solution frequency of CD_4 this decrease amounts to an extra red shift of about 2 cm^{-1} relative to the solid solution shift of CH_4 (Table V; cases 1, 3, 5, 7, 9, 11). Experimentally we observe for CD_4 a red shift of 3 cm^{-1} compared to a blue shift of 0.5 cm^{-1} for CH_4. Half of this difference is accounted for. There is another effect which produces a relative red shift of CD_4. This is the weak coupling between, for example, the frequencies of CH_4 and the frequencies of CD_4 of the host lattice. This will push the energy levels of CH_4 to higher energies. Similarly the levels of CD_4 in a host lattice of CH_4 will be pushed to lower energies.

A simple model of one C-H bond in between C-D bonds or vice versa results in:

$$\begin{aligned} \nu_H^o - \nu_H &= 4\left\{(\Delta\nu_{coupling})^2/\nu_H\right\}(1 - \mu_H/\mu_D)^{-1} \\ \nu_D^o - \nu_D &= 4\left\{(\Delta\nu_{coupling})^2/\nu_D\right\}(1 - \mu_D/\mu_H)^{-1}, \end{aligned} \tag{18}$$

where ν^o denotes the frequency without this particular effect and $\Delta\nu_{coupling}$ is the coupling splitting defined in Equation (5). Substituting in (18) the observed values for $\Delta\nu_{coupling}$ yields shifts in the bending region of -0.05 cm^{-1} and 0.16 cm^{-1} for CH_4 and CD_4 respectively which account for only a fraction of the difference in the measured shifts.

In the stretching region the difference between the observed solid solution shifts of CH_4 and CD_4 cannot be explained by Equations (17,18).

The observed splittings in the CD_4 bending region are about 15 °/o larger than in the CH_4 spectrum. In order to obtain this result the intermolecular force constants associated with the splitting in the CD_4 spectrum must be about 50 °/o larger than the corresponding force constants in CH_4. This difference must be caused by mass effects.

The first mass effect we consider here involves the movements of carbon atoms--up till now neglected--which are relatively more important in CD_4 than in CH_4. A consequence of the carbon recoil during a normal vibration is a decrease of the movements of hydrogens with respect to a coordinate system fixed

in the crystal. For the in-phase crystal modes the carbon movements will not influence intermolecular interactions and hence will not affect the spacing between E_+ and B_2. Therefore this qualitative explanation fails to account for the increased splitting observed in the CD_4 spectrum. (For the out-of-phase crystal modes recoil will cause a decrease of the atom-atom interactions and consequently a decrease of the spacing between E_+ and E_-).

Another mass effect is the change in the crystal dimensions because of the difference in the zero point amplitudes of CH_4 and CD_4. Also one might consider the change in each C-H bond length upon isotopic substitution. This arises from the difference in the zero-point energy levels of CH_4 and CD_4 together with the anharmonicity in the (common) intramolecular potential curve. However, the latter two mass effects are known to be small and it does not seem likely that they are respo[illegible]e for the increase of 50 $^0/_0$ in the intermolecular force constants in going from CH_4 to CD_4.

ACKNOWLEDGMENT

We should like to acknowledge the support of The Office of Naval Research.

TABLE II

Values for the First and Second Derivatives of the Hydrogen-Hydrogen Potential in Methane Crystals (Units: dyne $\times 10^{-8}$ and dyne cm^{-1} Respectively)

	Repulsive Potential				Attractive Potential		Electrostatic Potential	
	de Boer		Muller					
R_{ij}	$\frac{\partial V_R}{\partial R_{ij}}$	$\frac{\partial^2 V_R}{\partial R^2_{ij}}$	$\frac{\partial V_{R'}}{\partial R_{ij}}$	$\frac{\partial^2 V_{R'}}{\partial R^2_{ij}}$	$\frac{\partial V_A}{\partial R_{ij}}$	$\frac{\partial^2 V_A}{\partial R^2_{ij}}$	$\frac{\partial V_E}{\partial R_{ij}}$	$\frac{\partial^2 V_E}{\partial R^2_{ij}}$
2.77	-235	832	-216	1079	164	-416	-301	217
3.13	-65	229	-35	173	69	-155	-235	150
4.06	-3	9	0	2	11	-20	-140	69
4.13	-2	7	0	1	10	-17	-135	65
4.25	-1	4			8	-13	-128	60
4.50	-1	2			6	-9	-114	51
4.74	0	1			4	-6	-103	44
5.18					2	-3	-86	33
5.57					1	-2	-75	27
5.80					1	-1	-69	24

TABLE III

Values for the First and Second Derivatives of the Hydrogen-Carbon Potential in Methane Crystals (Units: dyne $\times 10^{-8}$ and dyne cm^{-1} Respectively)

	Repulsive Potential				Attractive Potential		Electrostatic Potential	
	de Boer		Muller					
R_{ik}	$\frac{\partial V_R}{\partial R_{ik}}$	$\frac{\partial^2 V_R}{\partial R_{ik}^2}$	$\frac{\partial V_{R'}}{\partial R_{ik}}$	$\frac{\partial^2 V_{R'}}{\partial R_{ik}^2}$	$\frac{\partial V_A}{\partial R_{ik}}$	$\frac{\partial^2 V_A}{\partial R_{ik}^2}$	$\frac{\partial V_E}{\partial R_{ik}}$	$\frac{\partial^2 V_E}{\partial R_{ik}^2}$
3.06	-143	558	-112	517	208	-477	987	-645
3.61	-17	65	-9	40	65	-126	708	-392
3.82	-7	29	-3	15	44	-81	634	-332
4.09	-3	10	-1	4	27	-47	552	-270
4.45	-1	3			15	-24	467	-210
4.68					11	-16	421	-180
4.84					8	-12	393	-162
4.99							371	-149
5.21							340	-130
5.29							330	-125
5.94							261	-88

TABLE IV A

Intermolecular Force Constants in Solid Methane* (Units: dyne cm^{-1})

Bending Region	Repulsive Forces		Attractive Forces	Electrostatic Forces	Total
	de Boer	Muller			a) de Boer b) Muller
Solid solution shift	1356+92	1400+60	-900-220	1398-1210	a) 414
	-343-54	-281-39	302+114	-1434+1313	
z	1051	1140	-704	67	b) 503
Solid solution shift	1613+112	1725+68	-1029-263	1467-1255	a) 560
	-317- 53	-258-40	284+108	-1399+1292	
x, y	1355	1495	-900	105	b) 700
Crystal shift	1149+92	1244+60	-749-220	1155-1210	a) 468
	-317-54	-158-39	262+114	-1067+1313	
z	870	1107	-593	191	b) 705
Crystal shift	1116+112	1357+68	-655-263	865-1255	a) 51
	-310- 53	-255-40	253+108	-1159+1292	
x, y	865	1130	-557	257	b) 316
Coupling splitting	-425	-381	305	-487	a) -3
	206	190	-155	551	
z	-219	-191	150	64	b) 25
Coupling splitting	-208	-273	156	-381	a) 242
	182	151	-156	649	
x, y	-26	-122	0	268	b) 146

*See footnote in TABLE IV B.

TABLE IV B

Intermolecular Force Constants in Solid Methane* (Units: dyne cm^{-1})

Stretching Region	Repulsive Forces		Attractive Forces	Electrostatic Forces	Total
	de Boer	Muller			a) de Boer b) Muller
Solid solution shift	1790+548 -294- 15	2135+502 -227- 8	-1053-502 280+ 71	1391-1350 -1436+1307	a) 737
x, y, z	2029	2402	-1204	-88	b) 1110
Crystal shift	1788+548 -293- 15	2135+502 -227- 8	-1049-502 268+ 71	1347-1350 -1198+1307	a) 922
z	2028	2402	-1212	106	b) 1296
Crystal shift	1735+548 -283- 15	2105+502 -222- 8	-984-502 263+ 71	1161-1350 -1282+1307	a) 669
x, y	1985	2377	-1152	-164	b) 1061
Coupling splitting	372 68	-400 68	243 -51	-376 212	a) -276
z	-304	-332	192	-164	b) -304
Coupling splitting	74 25	67 12	-16 -39	-149 295	a) 190
x, y	99	79	-55	146	b) 170

*The four entries are arranged as follows

Upper left: $(\partial^2 V^{HH}/\partial R_{ij}^2)\ (\partial R_{ij}/\partial S)^2$

Lower left: $(\partial V^{HH}/\partial R_{ij})\ (\partial^2 R_{ij}/\partial S^2)$

Upper right: $(\partial^2 V^{HC}/\partial R_{ik}^2)\ (\partial R_{ik}/\partial S)^2$

Lower right: $(\partial V^{HC}/\partial R_{ik})\ (\partial^2 R_{ik}/\partial S^2)$

TABLE V

Shifts and Splittings for Various Combinations of the Three Intermolecular Interactions V_R^*, V_A and V_E in Solid Methane (All Entries in cm^{-1})

	Interaction	BENDING REGION				STRETCHING REGION		
		Solid Solution Shift $(x,y+z)/2$	Site Splitting $x,y-z$	Coupling Splitting B_2-E_+	Coupling Splitting E_+-E_-	Solid Solution Shift $(x,y+z)/2$	Coupling Splitting B_2-E_+	Coupling Splitting E_+-E_-
1	$V_R+V_A+V_E$	7.6	2.2	2.6	7.5	2.2	-0.6	1.1
2	$V_R+2V_A+V_E$	-4.9	-0.7	4.4	7.5	-1.4	0.1	0.8
3	$V_R+V_A+2V_E$	8.9	2.8	6.5	15.9	2.0	-0.7	2.0
4	$V_R+2V_A+2V_E$	-3.5	-0.1	8.2	15.9	-1.7	-0.2	1.7
5	$V_{R'}+V_A+V_E$	9.4	3.0	4.1	4.5	3.4	-0.7	1.0
6	$V_{R'}+2V_A+V_E$	-3.1	0.0	5.9	4.5	-0.3	-0.1	0.7
7	$V_{R'}+V_A+2V_E$	10.7	3.6	6.4	12.9	3.1	-0.8	1.9
8	$V_{R'}+2V_A+2V_E$	-1.8	0.6	9.7	12.9	-0.5	-0.2	1.6
9	$V_R+V_A+V_E/2$	6.9	1.9	0.8	3.3	2.4	-0.6	0.7
10	$V_R+2V_A+V_E/2$	-5.5	-1.0	2.5	3.3	-1.3	0.0	0.3
11	$V_{R'}+V_A+V_E/2$	8.7	2.7	2.3	0.3	3.5	-0.6	0.6
12	$V_{R'}+2V_A+V_E/2$	-3.8	0.0	4.2	0.3	-0.1	-0.1	0.2
CH_4	Observed	0.5	<3	-3.9	4.1	-7.6	<4	<4
CD_4	Observed	-3.9	<1	-4.3	4.9	-7.2	<4	<4

APPENDIX I

The [U'] Matrix for Molecular Methane

	$S(A_1^{st})$	$S(F_x^{st})$	$S(F_y^{st})$	$S(F_z^{st})$	$S(F_x^{bd})$	$S(F_y^{bd})$	$S(F_z^{bd})$	$S(E_a^{bd})$	$S(E_b^{bd})$	$S(A_1^{bd})$
Δr_1	2^{-1}	2^{-1}	2^{-1}	2^{-1}						
Δr_2	2^{-1}	-2^{-1}	-2^{-1}	2^{-1}						
Δr_3	2^{-1}	2^{-1}	-2^{-1}	-2^{-1}						
Δr_4	2^{-1}	-2^{-1}	2^{-1}	-2^{-1}						
$\Delta\alpha_{12}d$					0	0	$2^{-1/2}$	$3^{-1/2}$	0	$6^{-1/2}$
$\Delta\alpha_{34}d$					0	0	$-2^{-1/2}$	$3^{-1/2}$	0	$6^{-1/2}$
$\Delta\alpha_{13}d$					$2^{-1/2}$	0	0	$-12^{-1/2}$	-2^{-1}	$6^{-1/2}$
$\Delta\alpha_{24}d$					$-2^{-1/2}$	0	0	$-12^{-1/2}$	-2^{-1}	$6^{-1/2}$
$\Delta\alpha_{14}d$					0	$2^{-1/2}$	0	$-12^{-1/2}$	2^{-1}	$6^{-1/2}$
$\Delta\alpha_{23}d$					0	$-2^{-1/2}$	0	$-12^{-1/2}$	2^{-1}	$6^{-1/2}$

APPENDIX II

The [D] Matrix for Molecular Methane*

Internal Coordinates	Normalization Factor	Δx_1	Δy_1	Δz_1	Δx_2	Δy_2	Δz_2	Δx_3	Δy_3	Δz_3	Δx_4	Δy_4	Δz_4
Δr_1	$3^{-1/2}$	1	1	1	0	0	0	0	0	0	0	0	0
Δr_2	$3^{-1/2}$	0	0	0	-1	-1	1	0	0	0	0	0	0
Δr_3	$3^{-1/2}$	0	0	0	0	0	0	1	-1	-1	0	0	0
Δr_4	$3^{-1/2}$	0	0	0	0	0	0	0	0	0	-1	1	-1
$\Delta\alpha_{12}d$	$6^{-1/2}$	1	1	-2	-1	-1	-2	0	0	0	0	0	0
$\Delta\alpha_{34}d$	$6^{-1/2}$	0	0	0	0	0	0	1	-1	2	-1	1	2
$\Delta\alpha_{13}d$	$6^{-1/2}$	-2	1	1	0	0	0	-2	-1	-1	0	0	0
$\Delta\alpha_{24}d$	$6^{-1/2}$	0	0	0	2	-1	1	0	0	0	2	1	-1
$\Delta\alpha_{14}d$	$6^{-1/2}$	1	-2	1	0	0	0	0	0	0	-1	-2	-1
$\Delta\alpha_{23}d$	$6^{-1/2}$	0	0	0	-1	2	1	1	2	-1	0	0	0

*Six rows for the conditions of no translation and rotation are omitted; so are the columns for the three coordinates of the carbon atom and one for the redundancy condition.

APPENDIX III

First Derivatives of the Intermolecular Hydrogen Distances in Crystalline Methane*

Neighbor Hydrogen	j	R_{ij}	$\frac{\partial R_{ij}}{\partial r_i}$	$\frac{\partial R_{ij}}{\partial r_j}$	$\frac{\partial R_{ij}}{d}^{-1}$ / $\partial\theta_{12}$	$\frac{\partial R_{ij}}{d}^{-1}$ / $\partial\theta_{13}$	$\frac{\partial R_{ij}}{d}^{-1}$ / $\partial\theta_{12}$ or $\frac{\partial R_{ij}}{d}^{-1}$ / $\partial\theta_{34}$	$\frac{\partial R_{ij}}{d}^{-1}$ / $\partial\theta_{13}$ or $\frac{\partial R_{ij}}{d}^{-1}$ / $\partial\theta_{24}$
q4	1	2.77	-0.944	-0.083	0.066	-0.312	0.675	0.297
q3	2	2.77	-0.944	-0.083	0.066	0.246	0.675	-0.972
(q-a)3	3	2.77	-0.083	-0.944	0.675	-0.972	0.066	0.246
(q-b)4	4	2.77	-0.083	-0.944	0.675	0.297	0.066	-0.312
q2	5	3.13	-0.834	0.242	0.552	-0.276	-0.970	0.485
(q-c)2	6	3.13	0.242	-0.834	-0.970	0.485	0.552	-0.276
(p+a)2	7	3.13	-0.296	-0.296	-0.209	0.912	-0.209	0.912
(p+a)4	8	3.13	-0.296	-0.296	-0.703	0.912	-0.703	0.912
(p+b)2	9	3.13	-0.296	-0.296	-0.209	-0.703	-0.209	-0.703
(p+b)3	10	3.13	-0.296	-0.296	-0.703	-0.209	-0.703	-0.209
(p+a+b)2	11	4.06	-0.816	-0.816	-0.577	0.289	-0.577	0.289
q1	12	4.13	-0.986	0.986	0.169	-0.085	-0.169	0.085
(q-c)1	13	4.13	-0.169	0.169	-0.986	0.493	0.986	-0.493
(q-b)1	14	4.13	-0.408	0.408	0.577	0.324	-0.577	-0.324
(q-b-c)1	15	4.13	0.408	-0.408	-0.577	0.901	0.577	-0.901
(q-a-b)1	16	4.13	0.169	-0.169	0.986	-0.493	-0.986	0.493
(q-a-b-c)1	17	4.13	0.986	-0.986	-0.169	0.085	0.169	-0.085
(q-a)1	18	4.13	-0.408	0.408	0.577	-0.901	-0.577	0.901
(q-a-c)1	19	4.13	0.408	-0.408	-0.577	-0.324	0.577	0.324
(p+a)1	20	4.13	-0.577	0.577	-0.408	0.816	0.408	-0.816
(p-b)1	21	4.13	0.577	-0.577	0.408	0.408	-0.408	-0.408
(p-a)1	22	4.13	0.577	-0.577	0.408	-0.816	-0.408	0.816
(p+b)1	23	4.13	-0.577	0.577	-0.408	-0.408	0.408	0.408

APPENDIX III (Continued)

First Derivatives of the Intermolecular Hydrogen Distances in Crystalline Methane*

Neighbor Hydrogen	j	R_{ij}	$\frac{\partial R_{ij}}{\partial r_i}$	$\frac{\partial R_{ij}}{\partial r_j}$	$\frac{\partial R_{ij_d}{}^{-1}}{\partial \theta_{12}}$	$\frac{\partial R_{ij_d}{}^{-1}}{\partial \theta_{13}}$	$\frac{\partial R_{ij_d}{}^{-1}}{\partial \theta_{12}}$ or $\frac{\partial R_{ij_d}{}^{-1}}{\partial \theta_{34}}$	$\frac{\partial R_{ij_d}{}^{-1}}{\partial \theta_{13}}$ or $\frac{\partial R_{ij_d}{}^{-1}}{\partial \theta_{24}}$
(q-b)3	24	4.25	-0.054	0.507	0.439	0.557	0.836	-0.237
(q-a)4	25	4.25	-0.054	0.507	0.439	-0.996	0.836	-0.599
(q-a-b)3	26	4.25	0.507	-0.054	0.836	-0.237	0.439	0.557
(q-a-b)4	27	4.25	0.507	-0.054	0.836	-0.599	0.439	-0.996
(q-b)2	28	4.50	-0.051	0.699	0.759	0.182	-0.301	0.712
(q-b-c)2	29	4.50	0.699	-0.051	-0.301	0.712	0.759	0.182
(q-a)2	30	4.50	-0.051	0.699	0.759	-0.941	-0.301	-0.411
(q-a-c)2	31	4.50	0.699	-0.051	-0.301	-0.411	0.759	-0.941
(p+a)3	32	4.50	-0.206	0.854	-0.489	0.979	0.260	-0.520
(p+b)4	33	4.50	-0.206	0.854	-0.489	-0.489	0.260	0.260
(p-a)3	34	4.50	0.854	-0.206	0.260	-0.520	-0.489	0.979
(p-b)4	35	4.50	0.854	-0.206	0.260	0.260	-0.489	-0.489
(q-c)3	36	4.73	0.161	0.664	-0.969	0.647	-0.613	-0.065
(q-c)4	37	4.73	0.161	0.664	-0.969	0.322	-0.613	0.678
(q-b-c)4	38	4.73	0.664	0.161	-0.613	0.678	-0.969	0.322
(q-a-c)3	39	4.73	0.664	0.161	-0.613	-0.065	-0.969	0.647
(p+a+b)3	40	5.18	-0.639	0.281	-0.750	0.524	-0.099	-0.777
(p+a+b)4	41	5.18	-0.639	0.281	-0.750	0.225	-0.099	0.876
(p+a-b)4	42	5.18	0.281	-0.639	-0.099	0.876	-0.750	0.225
(p-a+b)3	43	5.18	0.281	-0.639	-0.099	-0.777	-0.750	0.524
(p-a)2	44	5.54	0.694	0.694	0.491	-0.702	0.491	-0.702
(p-b)2	45	5.54	0.694	0.694	0.491	0.211	0.491	0.211
(p-a)4	46	5.54	0.694	0.694	0.211	-0.702	0.211	-0.702
(p-b)3	47	5.54	0.694	0.694	0.211	0.491	0.211	0.491

APPENDIX III (Continued)

First Derivatives of the Intermolecular Hydrogen Distances in Crystalline Methane*

Neighbor Hydrogen	j	R_{ij}	$\frac{\partial R_{ij}}{\partial r_i}$	$\frac{\partial R_{ij}}{\partial r_j}$	$\frac{\partial R_{ij_d}{}^{-1}}{\partial \theta_{12}}$	$\frac{\partial R_{ij_d}{}^{-1}}{\partial \theta_{13}}$	$\frac{\partial R_{ij_d}{}^{-1}}{\partial \theta_{12}}$ or $\frac{\partial R_{ij_d}{}^{-1}}{\partial \theta_{34}}$	$\frac{\partial R_{ij_d}{}^{-1}}{\partial \theta_{13}}$ or $\frac{\partial R_{ij_d}{}^{-1}}{\partial \theta_{24}}$
(q-a-b)2	48	5.54	0.390	0.998	0.921	-0.461	0.060	-0.030
(q-a-b-c)2	49	5.54	0.998	0.390	0.060	-0.030	0.921	-0.461
(q+a)4	50	5.60	-0.893	-0.466	-0.269	0.447	0.033	0.749
(q+b)3	51	5.60	-0.893	-0.466	-0.269	-0.179	0.033	-0.782
(q+a-b)4	52	5.60	-0.466	-0.893	0.033	0.749	-0.269	0.447
(q-a+b)3	53	5.60	-0.466	-0.893	0.033	-0.782	-0.269	-0.179
(q-b-c)3	54	5.73	0.549	0.965	-0.506	0.829	-0.212	0.241
(q-a-b-c)3	55	5.73	0.965	0.549	-0.212	0.241	-0.506	0.829
(q-a-b-c)4	56	5.73	0.965	0.549	-0.212	-0.029	-0.506	-0.323
(q-a-c)4	57	5.73	0.549	0.965	-0.506	-0.323	-0.212	-0.029
(q+b)2	58	5.79	-0.863	-0.281	0.007	-0.441	-0.816	-0.029
(q+a)2	59	5.79	-0.863	-0.281	0.007	0.434	-0.816	0.845
(q+b-c)2	60	5.79	-0.281	-0.863	-0.816	-0.029	0.007	-0.441
(q+a-c)2	61	5.79	-0.281	-0.863	-0.816	0.845	0.007	0.434
(p+a+b)1	62	5.84	-0.816	0.816	-0.577	0.289	0.577	-0.289
(p+a-b)1	63	5.84	0	0	0	0.866	0	-0.866
(p-a-b)1	64	5.84	0.816	-0.816	0.577	-0.289	-0.577	0.289
(p-a+b)1	65	5.84	0	0	0	-0.866	0	0.866
+(p-c)1	66	5.84	0.577	-0.577	-0.816	0.408	0.816	-0.408
+(p+c)1	67	5.84	-0.577	0.577	0.816	-0.408	-0.816	0.408
+(p+c)3	68	4.75	-0.403	-0.403	0.896	-0.285	0.896	-0.285
+(p+c)4	69	4.75	-0.403	-0.403	0.896	-0.611	0.896	-0.611

*Δr_i and $\Delta\theta$d are normal displacements of atom p1, while Δr_j and $\Delta\theta$'d are normal displacements of hydrogens in neighboring molecules.
+not indicated in Figure 2

APPENDIX IV

Second Derivatives of the Intermolecular Hydrogen Distances in Crystalline Methane*

Neighbor Hydrogen	j	$\frac{\partial^2 R_{ij}}{\partial r_i^2}$	$\frac{\partial^2 R_{ij}}{\partial r_i \partial r_j}$	$\frac{\partial^2 R_{ij}}{\partial \theta_{i2}^2} d^{-2}$	$\frac{\partial^2 R_{ij}}{\partial \theta_{i3}^2} d^{-2}$	$\frac{\partial^2 R_{ij}}{\partial \theta_{12} \partial \theta_{i2}} d^{-2}$ or $\frac{\partial^2 R_{ij}}{\partial \theta_{12} \partial \theta_{34}} d^{-2}$	$\frac{\partial^2 R_{ij}}{\partial \theta_{13} \partial \theta_{i3}} d^{-2}$ or $\frac{\partial^2 R_{ij}}{\partial \theta_{13} \partial \theta_{24}} d^{-2}$
q4	1	0.039	0.092	0.360	0.326	0.225	0.274
q3	2	0.039	0.092	0.360	0.339	0.225	-0.034
(q-a)3	3	0.359	0.092	0.197	0.020	0.225	-0.034
(q-a)4	4	0.359	0.092	0.197	0.330	0.225	0.274
q2	5	0.097	0.171	0.222	0.295	0.065	0.255
(q-c)2	6	0.300	0.171	0.019	0.244	0.065	0.255
(p+a)2	7	0.291	0.078	0.305	0.054	-0.120	-0.053
(p+a)4	8	0.291	0.078	0.162	0.054	0.055	-0.053
(p+b)2	9	0.291	0.078	0.305	0.162	-0.120	0.055
(p+b)3	10	0.291	0.078	0.162	0.305	0.055	-0.120
(p+a+b)2	11	0.082	-0.082	0.164	0.226	-0.164	0.144
q1	12	0.007	-0.007	0.235	0.240	-0.235	-0.240
(q-c)1	13	0.235	-0.235	0.007	0.183	-0.007	-0.183
(q-b)1	14	0.202	-0.202	0.162	0.217	-0.162	-0.217
(q-b-c)1	15	0.202	-0.202	0.162	0.046	-0.162	-0.046
(q-a-b)1	16	0.235	-0.235	0.007	0.183	-0.007	-0.183
(q-a-b-c)1	17	0.007	-0.007	0.235	0.240	-0.235	-0.240
(q-a)1	18	0.202	-0.202	0.162	0.046	-0.162	-0.046
(q-a-c)1	19	0.202	-0.202	0.162	0.217	-0.162	-0.217
(p+a)1	20	0.162	-0.162	0.202	0.081	-0.202	-0.081
(p-b)1	21	0.162	-0.162	0.202	0.202	-0.202	-0.202
(p-a)1	22	0.162	-0.162	0.202	0.081	-0.202	-0.081
(p+b)1	23	0.162	-0.162	0.202	0.202	-0.202	-0.202

APPENDIX IV (Continued)

Second Derivatives of the Intermolecular Hydrogen Distances in Crystalline Methane*

Neighbor Hydrogen	j	$\frac{\partial^2 R_{ij}}{\partial r_i^2}$	$\frac{\partial^2 R_{ij}}{\partial r_i \partial r_j}$	$\frac{\partial^2 R_{ij}}{\partial \theta_{12}^2} d^{-2}$	$\frac{\partial^2 R_{ij}}{\partial \theta_{13}^2} d^{-2}$	$\frac{\partial^2 R_{ij}}{\partial \theta_{12} \partial \theta_{12}'} d^{-2}$ or $\frac{\partial^2 R_{ij}}{\partial \theta_{12} \partial \theta_{34}'} d^{-2}$	$\frac{\partial^2 R_{ij}}{\partial \theta_{13} \partial \theta_{13}'} d^{-2}$ or $\frac{\partial^2 R_{ij}}{\partial \theta_{13} \partial \theta_{24}'} d^{-2}$
(q-b)3	24	0.234	0.085	0.190	0.162	0.070	-0.047
(q-a)4	25	0.234	0.085	0.190	0.002	0.070	0.016
(q-a-b)3	26	0.175	0.085	0.071	0.222	0.070	-0.047
(q-a-b)4	27	0.175	0.085	0.071	0.151	0.070	0.016
(q-b)2	28	0.222	0.082	0.094	0.215	-0.058	0.119
(q-b-c)2	29	0.114	0.082	0.202	0.110	-0.058	0.119
(q-a)2	30	0.222	0.082	0.094	0.026	-0.058	0.062
(q-a-c)2	31	0.114	0.082	0.202	0.185	-0.058	0.062
(p+a)3	32	0.213	0.113	0.169	0.009	0.177	0.039
(p+b)4	33	0.213	0.113	0.169	0.169	0.177	0.177
(p-a)3	34	0.060	0.113	0.207	0.162	0.177	0.039
(p-b)4	35	0.060	0.113	0.207	0.207	0.177	0.177
(q-c)3	36	0.206	0.042	0.014	0.123	0.015	-0.062
(q-c)4	37	0.206	0.042	0.014	0.189	0.015	0.095
(q-b-c)4	38	0.118	0.042	0.139	0.114	0.015	0.095
(q-a-c)3	39	0.118	0.042	0.139	0.210	0.015	-0.062
(p+a+b)3	40	0.114	0.099	0.084	0.140	0.114	0.014
(p+a+b)4	41	0.114	0.099	0.084	0.183	0.114	0.091
(p+a-b)4	42	0.178	0.099	0.191	0.045	0.114	0.091
(p-a+b)3	43	0.178	0.099	0.191	0.076	0.114	0.014
(p-a)2	44	0.094	-0.027	0.137	0.092	-0.103	0.031
(p-b)2	45	0.094	-0.027	0.137	0.172	-0.103	0.112
(p-a)4	46	0.094	-0.027	0.172	0.092	0.112	0.031
(p-b)3	47	0.094	-0.027	0.172	0.137	0.112	-0.103

APPENDIX IV (Continued)

Second Derivatives of the Intermolecular Hydrogen Distances in Crystalline Methane*

Neighbor Hydrogen	j	$\frac{\partial^2 R_{ij}}{\partial r_i^2}$	$\frac{\partial^2 R_{ij}}{\partial r_i \partial r_j}$	$\frac{\partial^2 R_{ij}}{\partial \theta_{12}^2} d^{-2}$	$\frac{\partial^2 R_{ij}}{\partial \theta_{13}^2} d^{-2}$	$\frac{\partial^2 R_{ij}}{\partial \theta_{12} \partial \theta_{12}} d^{-2}$ or $\frac{\partial^2 R_{ij}}{\partial \theta_{12} \partial \theta_{34}} d^{-2}$	$\frac{\partial^2 R_{ij}}{\partial \theta_{13} \partial \theta_{13}} d^{-2}$ or $\frac{\partial^2 R_{ij}}{\partial \theta_{13} \partial \theta_{24}} d^{-2}$
(q-a-b)2	48	0.153	-0.010	0.027	0.142	-0.070	0.118
(q-a-b-c)2	49	0.001	-0.010	0.180	0.180	-0.070	0.118
(q+a)4	50	0.036	-0.015	0.166	0.143	0.121	0.059
(q+b)3	51	0.036	-0.015	0.166	0.173	0.121	0.070
(q+a-b)4	52	0.140	-0.015	0.178	0.078	0.121	0.059
(q-a+b)3	53	0.140	-0.015	0.178	0.069	0.121	0.070
(q-b-c)3	54	0.122	-0.034	0.130	0.054	0.098	-0.093
(q-a-b-c)3	55	0.012	-0.034	0.167	0.073	0.098	-0.093
(q-a-b-c)4	56	0.012	-0.034	0.167	0.174	0.098	0.115
(q-a-c)4	57	0.122	-0.034	0.130	0.156	0.098	0.115
(q+b)2	58	0.044	0.016	0.173	0.139	-0.056	0.113
(q+a)2	59	0.044	0.016	0.173	0.140	-0.056	0.052
(q+b-c)2	60	0.159	0.016	0.058	0.173	-0.056	0.113
(q+a-c)2	61	0.159	0.016	0.058	0.049	-0.056	0.052
(p+a+b)1	62	0.057	-0.057	0.114	0.157	-0.114	-0.157
(p+a-b)1	63	0.171	-0.171	0.171	0.043	-0.171	-0.043
(p-a-b)1	64	0.057	-0.057	0.114	0.157	-0.114	-0.157
(p-a+b)1	65	0.171	-0.171	0.171	0.043	-0.171	-0.043
+(p-c)1	66	0.114	-0.114	0.057	0.143	-0.057	-0.143
+(p+c)1	67	0.114	-0.114	0.057	0.143	-0.057	-0.143
+(p+c)3	68	0.176	0.036	0.041	0.194	-0.029	-0.087
+(p+c)4	69	0.176	0.036	0.041	0.132	-0.029	0.062

*Δr_i and $\Delta \theta d$ are normal displacements of atom p1, while Δr_j and $\Delta \theta' d$ are normal displacements of hydrogens in neighboring molecules.
+not indicated in Figure 2.

TABLE V

Shifts and Splittings for Various Combinations of the Three Intermolecular Interactions V_R^*, V_A and V_E in Solid Methane (All Entries in cm^{-1})

	Interaction	BENDING REGION				STRETCHING REGION		
		Solid Solution Shift	Site Splitting	Coupling Splitting		Solid Solution Shift	Coupling Splitting	
		$(x,y+z)/2$	$x,y-z$	B_2-E_+	E_+-E_-	$(x,y+z)/2$	B_2-E_+	E_+-E_-
1	$V_R+V_A+V_E$	7.6	2.2	2.6	7.5	2.2	-0.6	1.1
2	$V_R+2V_A+V_E$	-4.9	-0.7	4.4	7.5	-1.4	0.1	0.8
3	$V_R+V_A+2V_E$	8.9	2.8	6.5	15.9	2.0	-0.7	2.0
4	$V_R+2V_A+2V_E$	-3.5	-0.1	8.2	15.9	-1.7	-0.2	1.7
5	$V_{R'}+V_A+V_E$	9.4	3.0	4.1	4.5	3.4	-0.7	1.0
6	$V_{R'}+2V_A+V_E$	-3.1	0.0	5.9	4.5	-0.3	-0.1	0.7
7	$V_{R'}+V_A+2V_E$	10.7	3.6	6.4	12.9	3.1	-0.8	1.9
8	$V_{R'}+2V_A+2V_E$	-1.8	0.6	9.7	12.9	-0.5	-0.2	1.6
9	$V_R+V_A+V_E/2$	6.9	1.9	0.8	3.3	2.4	-0.6	0.7
10	$V_R+2V_A+V_E/2$	-5.5	-1.0	2.5	3.3	-1.3	0.0	0.3
11	$V_{R'}+V_A+V_E/2$	8.7	2.7	2.3	0.3	3.5	-0.6	0.6
12	$V_{R'}+2V_A+V_E/2$	-3.8	0.0	4.2	0.3	-0.1	-0.1	0.2
CH_4	Observed	0.5	<3	-3.9	4.1	-7.6	<4	<4
CD_4	Observed	-3.9	<1	-4.3	4.9	-7.2	<4	<4

APPENDIX VI

Values of $\sum_j (\partial R_{ij}/\partial \rho_i)^2$ for Crystalline Methane*

j	R_{ij}	Type	STRETCH x, y, z	BEND z	BEND x, y
1 - 4	2.77	q	1.796	0.920	1.191
5 - 10	3.13	p,q	1.107	2.322	2.513
11	4.06	p	0.666	0.333	0.084
12 - 23	4.13	p,q	4.000	4.000	4.000
24 - 27	4.25	q	0.520	1.783	1.717
28 - 35	4.50	p,q	2.526	1.948	3.129
36 - 39	4.73	q	0.934	2.630	0.987
40 - 43	5.18	p	0.974	1.146	1.697
44 - 49	5.54	p,q	3.066	1.424	1.485
50 - 53	5.60	q	2.028	0.146	1.405
54 - 57	5.73	q	2.464	0.602	1.373
58 - 61	5.79	q	1.648	1.332	1.097
62 - 67	5.84	p	2.000	2.000	2.000
68 - 69	4.75	p	0.324	1.606	0.454

*In each case the summation is extended over all terms for which $|R_{ij}|$ are equal.

APPENDIX VII

Values of $\sum_j (\partial R_{ij}/\partial \rho_i)(\partial R_{ij}/\partial \rho_j)$ for Crystalline Methane *

j	R_{ij}	Type of molecule	STRETCH z	STRETCH x, y	BEND z	BEND x, y
7 - 10	3.13	p	0	-0.175	-0.901	-2.114
11	4.06	p	0.666	-0.666	0.333	-0.084
20 - 23	4.13	p	-1.333	-1.333	-0.666	-1.667
32 - 35	4.50	p	0.704	0	0.509	-0.764
40 - 43	5.18	p	0.718	0	-0.297	-1.208
44 - 47	5.54	p	0	-0.963	0.393	-1.271
62 - 67	5.84	p	-2.000	-2.000	-2.000	-2.000
68 - 69	4.75	p	-0.325	0	-1.606	-0.292
1 - 4	2.77	q	-0.313	0	-0.178	-0.293
5 - 6	3.13	q	-0.404	0.404	-1.070	0.267
12 - 19	4.13	q	-2.667	-2.667	-3.333	-2.333
24 - 27	4.25	q	0.055	0	1.468	-1.457
28 - 31	4.50	q	-0.143	0.143	-0.914	-1.033
36 - 39	4.73	q	-0.429	0	-2.376	-1.041
48 - 49	5.54	q	0.778	-0.778	0.111	-0.027
50 - 53	5.60	q	-1.665	0	0.036	-0.399
54 - 57	5.73	q	-2.119	0	-0.429	0.380
58 - 61	5.79	q	0.970	-0.970	0.023	-0.759

* In each case the summation is extended over all terms for which $|R_{ij}|$ are equal; where necessary sums for p and q type molecules are given separately.

APPENDIX VIII

Values of $\sum_j \partial^2 R_{ij} / \partial \rho_i^2$ for Crystalline Methane *

(Units : $cm^{-1} \times 10^8$)

j	R_{ij}	Type of Molecule	STRETCH x, y, z	BEND z	BEND x, y
1 - 4	2.77	q	0.796	1.114	1.015
5 - 10	3.13	p,q	1.561	1.175	1.114
11	4.06	p	0.082	0.164	0.226
12 - 23	4.13	p,q	1.940	1.940	1.940
24 - 27	4.25	q	0.818	0.522	0.537
28 - 35	4.50	p,q	1.218	1.344	1.083
36 - 39	4.73	q	0.648	0.388	0.962
40 - 43	5.18	p	0.584	0.550	0.444
44 - 49	5.54	p,q	0.530	0.825	0.815
50 - 53	5.60	q	0.352	0.688	0.463
54 - 57	5.73	q	0.268	0.594	0.457
58 - 61	5.79	q	0.406	0.462	0.501
62 - 67	5.84	p	0.684	0.684	0.684
68 - 69	4.75	p	0.352	0.082	0.326

* In each case the summation is extended over all terms for which $|R_{ij}|$ are equal.

APPENDIX IX

Values of $\sum_j \partial^2 R_{ij}/\partial\rho_i\partial\rho_j$ for Crystalline Methane *

(Units : $cm^{-1} \times 10^8$)

j	R_{ij}	Type of molecule	STRETCH z	STRETCH x, y	BEND z	BEND x, y
7 - 10	3.13	p	0	-0.156	-0.350	-0.069
11	4.06	p	-0.082	0.082	-0.164	-0.144
20 - 23	4.13	p	-0.644	-0.644	-0.808	-0.566
32 - 35	4.50	p	-0.452	0	-0.708	-0.276
40 - 43	5.18	p	-0.396	0	-0.456	-0.154
44 - 47	5.54	p	0	0.054	-0.430	-0.277
62 - 67	5.84	p	-0.684	-0.684	-0.684	-0.684
68 - 69	4.75	p	-0.072	0	0.058	-0.149
1 - 4	2.77	q	-0.368	0	-0.900	-0.616
5 - 6	3.13	q	0.342	-0.342	0.130	-0.510
12 - 19	4.13	q	-1.292	-1.292	-1.128	-1.372
24 - 27	4.25	q	-0.340	0	-0.280	-0.126
28 - 31	4.50	q	0.328	-0.328	-0.232	-0.362
36 - 39	4.73	q	-0.168	0	-0.060	-0.314
48 - 49	5.54	q	-0.020	0.020	-0.140	-0.236
50 - 53	5.60	q	0.060	0	-0.484	0.022
54 - 57	5.73	q	0.136	0	-0.392	-0.416
58 - 61	5.79	q	0.064	-0.064	-0.224	-0.330

* In each case the summation is extended over all terms for which $|R_{ij}|$ are equal; where necessary sums for p and q type molecules are given separately.

Captions for the Figures

Figure 1 A. The absorption spectra of the low-temperature phase II of crystalline CH_4 and CD_4 in the ν_3 and ν_4 regions.

Figure 1 B. The absorption spectra in the ν_4 region of 2 °/o solutions of both isotopic species taken in phase II of the solvent species. The numbers inside the bands indicate the line width in cm^{-1}.

Figure 2. Schematic representation of the D_{2d}^2 crystal structure suggested for methane in phase II. The carbon atoms of type q molecules (indicated by a circle at the carbon atom) are 1/2 unit cell above or below plane of figure. Two edges of each tetrahedron are parallel to figure plane; the upper edge is shown as a solid line.

One face of the crystallographic unit cell (f.c.c.) is formed by the five molecules q, q±a, q±b. The primitive unit cell contains just the molecules p and q.

The lattice constant in the f.c.c. cell is h = 5.84 A. In the tetragonal unit cell the lattice constants are

$c = h = 5.84$ A and $a = b = h.2^{-1/2} = 4.13$ A

The intermolecular hydrogen contacts to atom p1 for which $R_{ij} < 6$A are indicated in the Figure. Hydrogens belonging to molecules q which are below plane of figure are marked with a circle.

$R_f = 2.77$ A
$R_g = 3.13$ A
$R_h = 4.06$ A
$R_k = 4.13$ A
$R_l = 4.25$ A
$R_m = 4.50$ A
$R_n = 4.73$ A
$R_o = 5.18$ A
$R_s = 5.54$ A
$R_t = 5.60$ A
$R_u = 5.73$ A
$R_v = 5.79$ A
$R_w = 5.84$ A

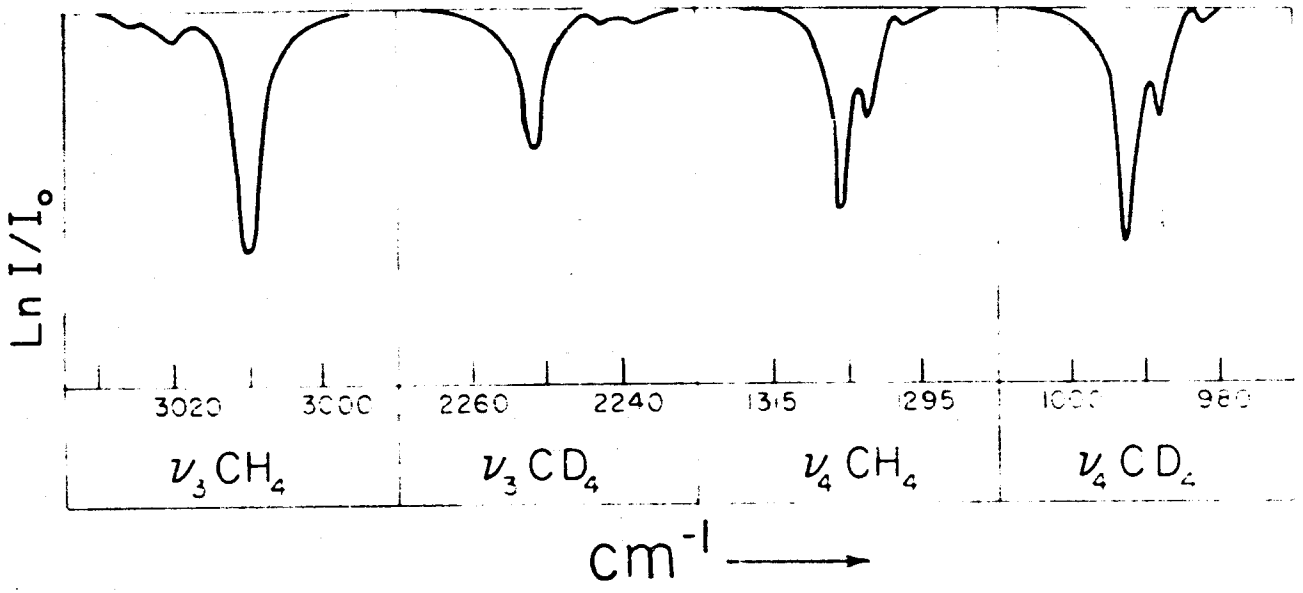
Ln I/I₀
3020
3000
2260
2240
1315
1295
1000
980
ν₃ CH₄
ν₃ CD₄
ν₄ CH₄
ν₄ CD₄
cm⁻¹

FIGURE 1a.

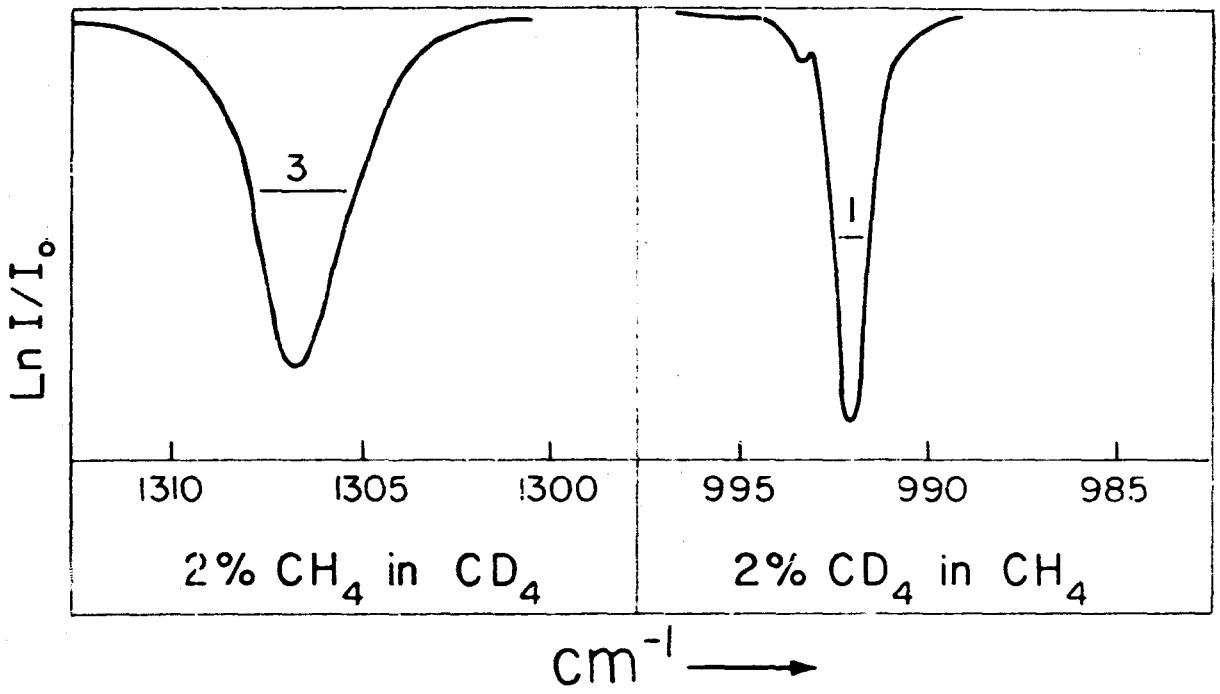

FIGURE 1b.

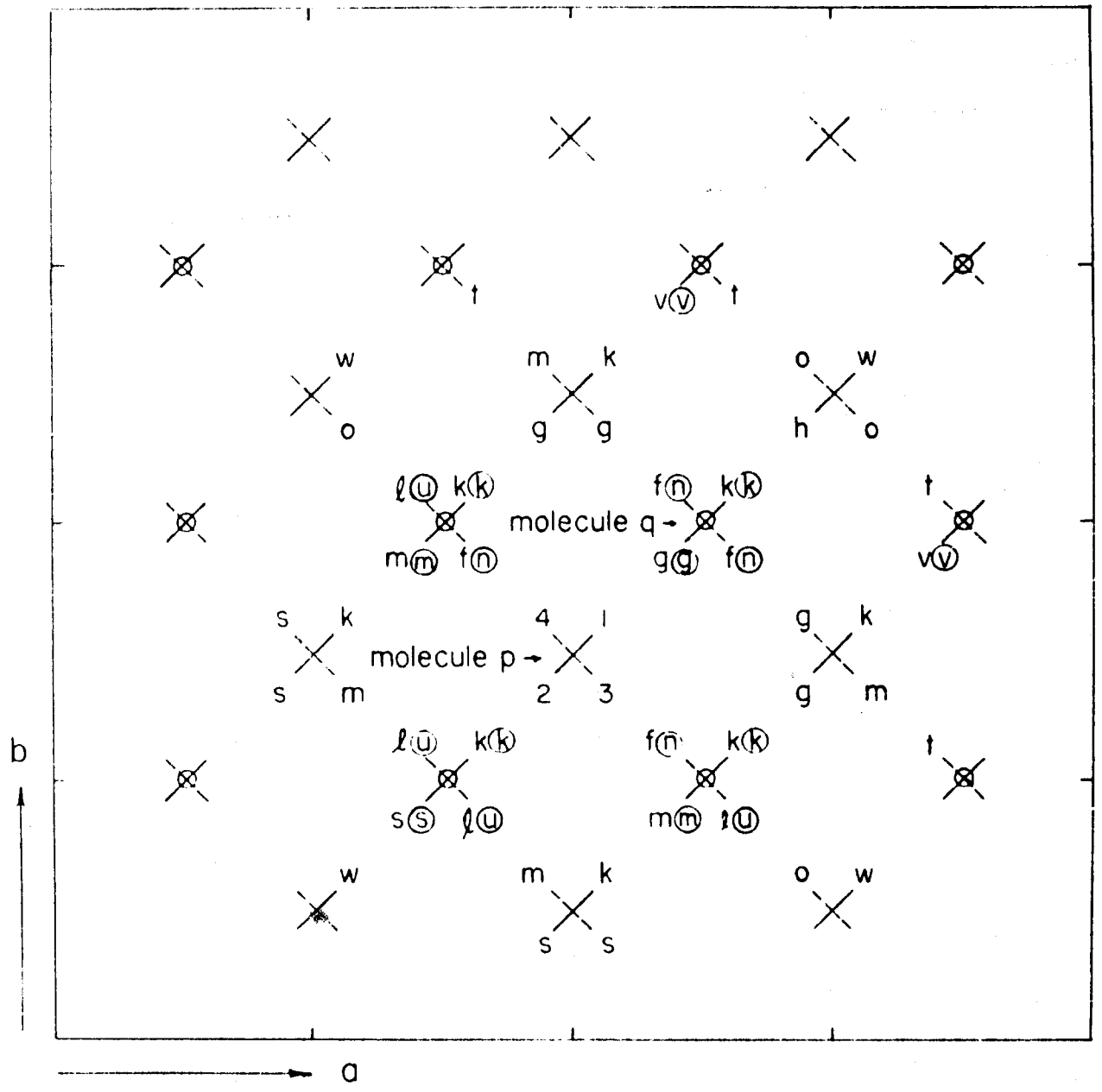

FIGURE 2.